Supporting Information

Improving Solar Cell Efficiency Through Hydrogen Bonding: A Method for Tuning the Active Layer Morphology

Taner Aytun,[⊥] Leonel Barreda,[⊥] Amparo Ruiz-Carretero, Jessica A. Lehrman and Samuel I. Stupp*

Table of Contents

Materials and Methods

Unless otherwise specified, all reagents were used without further purification. 2-phenylthiophene, butyllithium, tributyltin chloride, 2-butyl-1-octanol, p-tolunesulfonyl chloride, benzyl cyanoacetate, cyanoacetic acid, N-methylpiperazine, tetrakistriphenylphosphine palladium [$Pd(PPh_3)_4$], triphenylphosphine, anhydrous acetonitrile, anhydrous dimethylsulfoxide (DMSO), sodium azide, triethylamine (NEt_3) and piperidine (vacuum distilled over NaOH pellets and stored under nitrogen) were obtained from Sigma-Aldrich; 2-2-bithiophene carboxaldehyde was obtained from TLC America; N-benzyl-2-cyanoacetate was obtained from Santa Cruz Biotechnology; dimethylformamide (DMF), dichloromethane (DCM), hexanes, ethyl acetate (EtOAc) and hydrochloric acid (HCl) were obtained from Avantor Performance Materials; pyridine was obtained from Alfa Aesar; chloroform ($CHCl_3$), tetrahydrofuran (THF) and methanol (MeOH) were obtained from BDH; 1-Ethyl-3-(3-dimethylaminopropyl)carbodiimide (EDC) and hydroxybenzotriazole hydrate (HOBt) were obtained from Advanced Chemtech. 4-(Dimethylamino)pyridinium-4-toluenesulfonate (DPTS) was prepared according to previously published procedure. Anhydrous solvents were degassed on a Vacuum Atmospheres 103991 system. Proton NMR spectra were performed on a Varian Inova 500 or Agilent DD MR-400 with working frequencies of 500 and 400 Mhz, respectively. Carbon NMR spectra were obtained using a Bruker Avance III 500 spectrometer, with working frequency of 125.6 MHz for ^{13}C nuclei. Chemical shifts are reported in parts per million (ppm) and referenced to the residual nondeuterated solvent frequencies ($CDCl_3$: δ 7.26 ppm for ^{1}H, δ 77.36 ppm for ^{13}C). High-resolution mass spectra were recorded on an Agilent Model 6210 LC-TOF multimode ionization (MMI) or a Bruker Autoflex III MALDI mass spectrometers. Ultraviolet−visible (UV-vis) spectra were recorded on a Perkin Elmer LAMBDA 1050 spectrophotometer. Cyclic voltammetry was performed using an EG&G Princeton Applied Research Potentiostat (Model 263A), using a three- electrode system, with a Au disk working electrode, Pt wire counter electrode, a $Ag/AgNO_3$ non-aqeous reference electrode

(Bioanalytical Systems, Inc., models MF-2014, mF-2062 and MW-1032, repectively). Working electrodes were polished with a suspension of aluminum particles and on a nylon pad (Bioanalytical Systems, Inc. model MF-2060). Infrared spectra were obtained using a Thermo Nicolet, Nexus 870 spectrometer. Photovoltaic measurements were done while the devices were illuminated by an Oriel Xe solar simulator equipped with and Oriel 130 monochromator and a Keithley 2400 source meter. Filters were used to cut off grating overtones. The solar spectrum was simulated using an AM 1.5 filter with 100 mW/cm^2 power density. A calibrated silicon reference solar cell with a KG5 filter certified by the National Renewable Energy Laboratory was used to confirm the measurement conditions. AFM characterization was performed using a Bruker Dimension ICON atomic force microscope (Bruker Co.) at ambient conditions. Tapping mode was utilized with single-beam silicon cantilevers with a nominal oscillation frequency of 300 kHz. Conventional TEM of the samples were imaged using Hitachi HT-7700 TEM at 80-100 kV. 2D-GIXD measurements were performed at Beamline 8ID of the Advanced Photon Source at Argonne National Laboratory.[1] An x-ray wavelength of λ = 1.6868 Å was used and data were collected using a 1-2 s exposure at a sample-detector distance of 204 mm with a Pilatus photodiode array.

Synthesis

Synthesis of **1** has been reported elsewhere.[2]

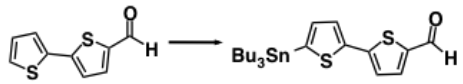

2

5'-(tributylstannyl)-2,2'-bithiophene-5-carbaldehyde (2) was synthesized using a modified procedure from the literature.[3] 2,2-Bithiophene-5-carboxaldehyde (0.5 g, 2.57 mmol) was placed in an oven-dried 250 mL Schlenk flask. The flask was degassed by three vacuum/nitrogen cycles. Anhydrous THF (30 mL) was injected and the solution was cooled to -78°C. N-methylpiperazine (0.313 mL, 2.83 mmol) was then injected, followed by n-butyllithium (1.13 mL, 2.5M in hexane, 2.83 mmol), after which the reaction was stirred for 20min. The reaction was then warmed to -20°C, followed by a second addition of *n*-butyllithium (1.13 mL, 2.5M in hexane, 2.83 mmol) and left stirring for another 30 min. Tributyltin chloride was then added (0.831 mL, 3.08 mmol) and the cooling bath was removed. After warming to room temperature, the reaction was quenched with 1 M HCl (20 mL). The crude was concentrated under vacuum, diluted in water (200 mL) and extracted with hexanes. The organic phase was separated and dried over magnesium sulfate ($MgSO_4$), followed by solvent removal under vacuum. Column chromatography in 1:1 DCM/hexanes afforded **5** as a yellow liquid (1.05 g, 85%). ^{1}H-NMR (500 MHz; $CDCl_3$): δ 9.85 (s, 1H), 7.66 (d, *J* = 4.0 Hz, 1H), 7.47 (d, *J* = 3.4 Hz, 1H), 7.25 (d, *J* = 4.0 Hz, 1H), 7.11 (d, *J* = 3.4 Hz, 1H), 1.61-1.54 (m, 6H), 1.35 (m, 6H), 1.15-1.12 (m, 6H), 0.91 (t, *J* = 7.3 Hz, 9H). ^{13}C-NMR (126 MHz; $CDCl_3$): δ 183.0, 147.9, 141.61, 141.53, 141.3, 137.9, 136.9, 127.6, 124.3, 29.3, 27.6, 14.0, 11.3 HRMS calc m/z for $C_{21}H_{32}OS_2Sn$: $[M+H]^+$ 485.0997, found 485.0993.

Compound 3. In a 250 mL oven-dried Schlenk flask, **1** (0.240 g, 0.302 mmol), **2** (0.321 g, 0.664 mmol) and tetrakistriphenylphosphine palladium(0) (0.068 g, 0.0601 mmol) were placed. The flask was then degassed by three vacuum/nitrogen cycles. Degassed DMF, 40 mL was then injected into the flask and the solution mixture was stirred for 12h at 120 °C under nitrogen. After cooling to room temperature, the reaction mixture was poured into water (300 mL) with brine (30 mL). The precipitate was filtered over Celite, washed with additional water (100 mL) and the Celite was then washed with DCM until the washings were faint blue color. Residual water was removed in a separatory funnel. DCM was removed under vacuum and the product was purified by column chromatography (100% DCM) to afford **2** as a dark green solid (0.229 g, 74%). ^{1}H-NMR (500 MHz; $CDCl_3$): δ 9.78 (s, 2H), 8.84 (d, *J* = 4.1 Hz, 2H), 7.59 (d, *J* = 3.9 Hz, 2H), 7.22 (d, *J* = 3.9 Hz, 4H), 7.17 (t, *J* = 4.5 Hz, 4H), 3.95 (d, *J* = 7.6 Hz, 4H), 1.87 (m, 2H), 1.27-1.17 (m, 36H), 0.82-0.77 (m, 12H). ^{13}C-NMR (126 MHz; $CDCl_3$): δ 182.7, 161.7, 146.4, 142.4, 141.8, 139.5, 137.9, 137.7, 137.1, 136.6, 129.2, 127.4, 126.3, 125.6, 124.8, 109.0, 46.6, 38.3, 32.2, 31.7, 31.4, 30.1, 28.9, 26.7, 23.5, 23.0, 14.5 HRMS calc m/z for $C_{56}H_{64}N_2O_4S_6$: 1020.319, found 1020.317.

S-Amide. 3 (0.120 g, 0.117 mmol) was placed in a 100 mL flask and dissolved in $CHCl_3$ (20 mL). **4** (0.074 g, 0.293 mmol) and piperidine (0.116 mL, 1.17 mmol) were then added and the solution was stirred at 70 °C for 12 h. After cooling to room temperature, the solution was diluted with DCM (100 mL) and washed with 1 M HCl (30 mL). The organic phase was collected and the solvent removed under vacuum. The product was purified by column chromatography (1%MeOH/ 1%Et_3N/ DCM) to afford S-Amide as a dark green solid (0. 080 g, 46%). ^{1}H-NMR (500 MHz; $CDCl_3$): δ 8.93 (d, *J* = 4.2 Hz, 2H), 8.34 (s, 2H), 7.61 (d, *J* = 4.2 Hz, 2H), 7.34 (t, *J* = 3.9 Hz, 4H), 7.27 (d, *J* = 3.9 Hz, 2H), 7.25 (d, *J* = 4.0 Hz, 2H), 6.23 (t, *J* = 5.8 Hz, 2H), 4.04 (d, *J* = 7.6 Hz, 4H), 3.35 (t, *J* = 6.0 Hz, 4H), 1.96 (m, 2H), 1.62-1.58 (m, 2H), 1.24 (m, 64H), 0.91 (m, 24H). ^{13}C-NMR (126 MHz; $CDCl_3$): δ 161.9, 160.8, 145.2, 144.3, 141.9, 139.6, 138.6, 137.9, 137.1, 136.6, 135.6, 129.3, 127.5, 126.5, 125.8, 125.0, 117.7, 109.1, 100.0, 46.7, 44.3, 38.3, 32.19, 32.17, 31.82, 31.65, 31.4, 30.08, 29.97, 29.2, 29.0, 27.0, 26.7, 23.47, 23.34, 23.02, 23.00, 14.48, 14.44 HRMS calc m/z for $C_{86}H_{116}N_6O_4S_6$ 1488.738, found 1490.736.

S-Ester. 3 (0.110 g, 0.108 mmol) was placed in a 100 mL flask and dissolved in $CHCl_3$ (20 mL). **5** (0.068mL, 0.268 mmol) and piperidine (0.106 mL, 1.08 mmol) were then added and the solution was stirred at 70 °C for 12 h. After cooling to room temperature, the solution was diluted with DCM (100 mL) and washed with 1 M HCl (30 mL). The organic phase was collected and the solvent removed under vacuum. The product was purified by column chromatography (DCM) to afford S-Ester as a dark green solid (0.120 g, 74%). ^{1}H-NMR (500 MHz; $CDCl_3$): δ 8.92 (d, *J* = 4.2 Hz, 2H), 8.21 (s, 2H), 7.64 (d, *J* = 4.1 Hz, 2H), 7.31 (d, *J* = 4.0 Hz, 2H), 7.28 (d, *J* = 4.1 Hz, 2H), 7.23 (d, *J* = 3.9 Hz, 4H), 4.19 (d, *J* = 5.8 Hz, 4H), 4.02 (d, *J* = 7.6 Hz, 4H), 1.95 (m, 2H), 1.76 (m, 2H), 1.34-1.24 (m, 64H), 0.88 (m, 24H). ^{13}C-NMR (126 MHz; $CDCl_3$): δ 163.4, 161.9, 146.6, 146.2, 141.8, 139.7, 139.3, 138.2, 137.1, 136.3, 135.2, 129.4, 127.8, 126.5, 125.7, 125.0, 116.1, 109.1, 98.5, 46.7, 38.3, 37.6, 32.2, 31.64, 31.51, 31.36, 31.18, 30.08, 29.95, 29.2, 28.9, 27.0, 26.7, 23.46, 23.31, 23.02, 23.00, 14.5 HRMS calc m/z for $C_{86}H_{114}N_4O_6S_6$1490.706, found 1490.707.

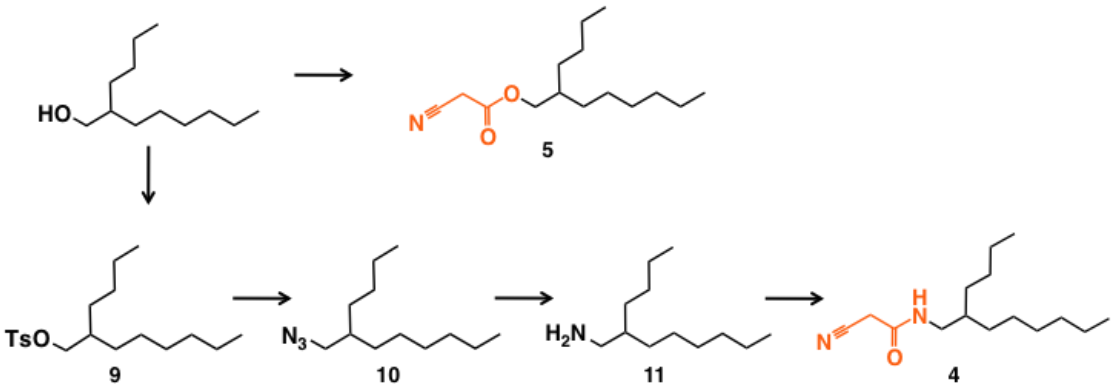

2-Butyloctyl 4-methylbenzenesulfonate (9). In a 250 mL flask, 2-butyl-1-octanol (20 g, 107 mmol) was dissolved in 40 mL of pyridine and cooled to 0 °C. *p*-Toluenesulfonyl chloride (19.4 g, 102 mmol) was then added and the solution was left stirring for 12 h. The crude was poured onto 150 mL of 4 M HCl and extracted with hexane. The organic phase was dried over $MgSO_4$, and the solvent was removed under vacuum to afford **7** as a colorless liquid (34.88g, 96%).^{1}H-NMR (500 MHz; $CDCl_3$): δ 7.79 (d, *J* = 8.3 Hz, 2H), 7.34 (d, *J* = 8.0 Hz, 2H), 3.91 (d, *J* = 5.3 Hz, 2H), 2.45 (s, 3H), 1.58 (m, 1H), 1.25-1.11 (m, 16H), 0.85 (m, 6H). ^{13}C-NMR (126 MHz; $CDCl_3$): δ 144.9, 133.4, 130.1, 128.3, 73.2, 37.9, 32.1, 30.9, 30.6, 29.8, 29.0, 26.8, 23.2, 23.0, 22.0, 14.45, 14.34 HRMS calc m/z for $C_{19}H_{32}O_3S$: $[M+Na]^+$ 363.1964, found 363.1964.

5-(azidomethyl)undecane (10). In a 100 mL flask, **9** (5 g, 14.68 mmol) was dissolved in DMSO (20 mL); sodium azide was then added (1.91 g, 29.4 mmol) and the solution was heated to 70 °C for 12 h. After cooling to room temperature, the crude was diluted with water (200 mL) and extracted with ethyl acetate. The organic phase was collected, dried over MgSO4, and the solvent was removed under

vacuum to afford **8** as a colorless liquid (3.10 g, 99%). ^{1}H-NMR (500 MHz; $CDCl_3$): δ 3.23 (d, *J* = 5.9 Hz, 2H), 1.55 (m, 1H), 1.28 (m, 16H), 0.91-0.88 (m, 6H). ^{13}C-NMR (126 MHz; $CDCl_3$): δ 55.3, 38.2, 31.85, 31.79, 31.5, 29.6, 28.9, 26.6, 23.0, 22.7, 14.15, 14.11 HRMS not possible due to sample fragmentation under several conditions. Elemental analysis: C: calc 68.20%, found 67.85±1.5 %; N: calc 19.88%, found 19.79±1.3%.

2-butyloctan-1-amine (11). In a 100 mL flask, **10** (3.10 g, 14.68 mmol) and triphenylphosphine (4.62 g, 17.6 mmol) were dissolved in THF (20 mL). The solution was heated at 70 °C for 12 h, then 5 mL of water were added and the solution was left stirring for another hour. After cooling to room temperature, the crude was concentrated under vacuum, diluted with water and extracted with DCM. The product was purified by column chromatography (5% MeOH/DCM, then 5% MeOH/ 5% NEt_3/ DCM) to afford **9** as a colorless liquid (2.44 g, 90%). ^{1}H-NMR (500 MHz; $CDCl_3$): δ 2.60 (d, *J* = 5.2 Hz, 2H), 1.45 (m, 2H), 1.26 (m, 16H), 0.91 (m, 6H). ^{13}C-NMR (126 MHz; CDCl3): δ 45.5, 41.1, 32.3, 31.9, 31.6, 31.3, 30.1, 29.3, 27.1, 23.5, 23.0, 14.5 HRMS calc m/z for $C_{12}H_{27}N$: $[M+H]^+$ 186.2223, found 186.2216.

***N*-(2-butyloctyl)-2-cyanoacetamide (4).** In a 250 mL flask, cyanoacetic acid (1.38 g, 16.1 mmol) was suspended in DCM (10 mL), then Et_3N (2.25 mL, 16.2 mmol) was added. Once all acid was dissolved, EDC, (3.1 g, 16.2 mmol) and HOBt (1.65 g, 16.2 mmol) were added in succession. After approximately one minute, a solution of **10** (2 g, 10.78 mmol) in DCM (5 mL) was added in one portion, after which the reaction was left stirring for 12 h. The crude was diluted with DCM, and extracted with water. After collecting the organic phase, the solvent was removed under vacuum and the product was purified by column chromatography (1% MeOH/DCM) to give 10 as a clear yellow liquid (2.55 g, 94%). ^{1}H-NMR (500 MHz; $CDCl_3$): δ 6.04 (s, 1H), 3.38 (s, 2H), 3.24 (t, *J* = 6.0 Hz, 2H), 1.53 (m, 1H), 1.27 (m, 16H), 0.89 (m, 6H). ^{13}C-NMR (126 MHz; CDCl3): δ 161.0, 115.2, 77.4, 44.0, 38.1, 32.13, 32.04, 31.7, 29.9, 29.1, 26.9, 26.2, 23.3, 23.0, 14.45, 14.40 HRMS calc m/z for $C_{15}H_{28}N_2O$: 252.2202, found 252.2199.

2-Butyloctyl 2-cyanoacetate (5). In a 250 mL flask, cyanoacetic acid (1.37 g, 16.1 mmol) was suspended in DCM (10 mL), then 4-(dimethylamino)pyridinium-4-toluenesulfonate (DPTS, 4.83 g, 16.1 mmol) was added. Once all acid was dissolved, EDC (3.09 g, 16.1 mmol) was added. After approximately one minute, a solution of 2-butyl-1-octanol (2 g, 10.73 mmol) in DCM (5 mL) was added in one portion, after which the reaction was left stirring for 12 h. The crude was diluted with DCM, and extracted with water. After collecting the organic phase, the solvent was removed under vacuum and the product was purified by column chromatography (20% EtOAc/hexane) to give **11** as a colorless liquid (2.60 g, 96%). ^{1}H-NMR (500 MHz; $CDCl_3$): δ 4.12 (d, *J* = 5.8 Hz, 2H), 3.46 (s, 2H), 1.67 (m, 1H), 1.34-1.27 (m, 16H), 0.89 (q, *J* = 7.0 Hz, 6H). ^{13}C-NMR (126 MHz; CDCl3): δ 163.4, 113.3, 77.4, 70.1, 37.5, 32.1, 31.3, 31.0, 29.9, 29.2, 26.9, 25.1, 23.3, 23.0, 14.45, 14.39 HRMS calc m/z for $C_{15}H_{27}NO_2$: $[M+Na]^+$ 276.1934, found 276.1931.

Compound 6. In a 250 mL oven-dried Schlenk flask, **1** (0.510 g, 0.642 mmol), **2** (0.310 g, 0.578 mmol) and tetrakistriphenylphosphine palladium(0) (0.073 g, 0.065 mmol) were placed. The flask was then degassed by three vacuum/nitrogen cycles. Degassed DMF (60 mL) was then injected into the flask and the solution mixture was stirred for 12h at 100 °C under nitrogen. After cooling to room temperature, the reaction mixture was poured into water (300 mL) with brine (30 mL). The precipitate was filtered over Celite, washed with additional water (100 mL) and the Celite was then washed with DCM until the washings were faint blue color. Residual water was removed in a separatory funnel. DCM was removed under vacuum and the product was purified by column chromatography (30%hexane/DCM) to afford **3** as a dark blue solid (0.230 g, 39%). ^{1}H-NMR (400 MHz; $CDCl_3$): δ 9.87 (s, 1H), 8.89 (d, *J* = 4.2 Hz, 1H), 8.61 (d, *J* = 4.2 Hz, 1H), 7.68 (d, *J* = 4.0 Hz, 1H), 7.32 (m, *J* = 11.7 Hz, 2H), 7.27 (d, *J* = 3.5 Hz, 1H), 7.25 (d, *J* = 4.2 Hz, 1H**)**, 7.21 (d, *J* = 4.2 Hz, 1H), 4.01 (d, *J* = 7.7 Hz, 2H), 3.94 (d, *J* = 7.8 Hz, 2H), 1.90 (m, 2H), 1.26 (m, 32H), 0.85 (m, 12H). ^{13}C-NMR (126 MHz; $CDCl_3$): δ 182.8, 161.87, 161.68, 146.4, 142.4, 142.0, 140.2, 139.2, 137.84, 137.66, 137.1, 136.7, 135.5, 131.7, 131.5, 129.1, 127.5, 126.4, 125.7, 124.9, 119.2, 108.70, 108.62, 46.64, 46.60, 38.3, 38.1, 32.17, 32.11, 31.62, 31.45, 31.33, 31.17, 30.07, 30.01, 28.90, 28.71, 26.66, 26.47, 23.44, 23.39, 23.0, 14.46, 14.39. HRMS calc m/z for $C_{47}H_{59}BrN_2O_3S_4$: 906.2592, found 906.2586.

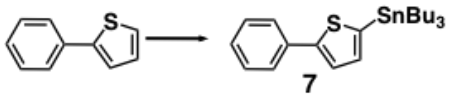

7

Tributyl(5-phenylthiophen-2-yl)stannane (7). 2-Phenylthiophene (0.5 g, 3.12 mmol) was placed in an oven-dried 100 mL Schlenk flask and degassed by three vacuum/nitrogen cycles. Anhydrous THF (30 mL) was injected and the solution was cooled to -78 °C. N-butyllithium (1.25 mL, 2.5M in hexanes, 3.12 mmol) was then injected, and the reaction was left stirring for 30 min. Tributyltin chloride (0.841 mL, 3.12 mmol) was then injected and the cooling bath was removed. After warming to room temperature, the reaction was quenched by adding water (5 mL). The crude was then concentrated under vacuum, diluted with water (200 mL), 1 M NaOH (50 mL) and extracted with hexanes. The organic phase was collected, dried under $MgSO_4$, followed by solvent removal under vacuum to afford **6** as a colorless liquid (1.35 g, 96%). This compound was found to be unstable to column chromatography; if isolated, this product should be used in subsequent steps without further purification. ^{1}H-NMR (500 MHz; $CDCl_3$): δ 7.63 (d, *J* = 7.2 Hz, 2H), 7.43 (d, *J* = 3.3 Hz, 1H), 7.36 (t, *J* = 7.8 Hz, 3H), 7.14 (d, *J* = 3.3 Hz, 1H), 1.59 (m, 6H), 1.36 (m, 6H), 1.14-1.11 (m, 6H), 0.89 (m, 9H). ^{13}C-NMR (126 MHz; $CDCl_3$): δ 150.3, 137.2, 136.8, 134.9, 129.22, 129.12, 127.4, 126.28, 126.25, 124.6, 77.4, 29.3, 27.6, 14.0, 11.2 HRMS calc m/z for $C_{22}H_{34}SSn$: 450.1403, found 450.1410.

Compound 8. 6 (0.230 g, 0.242 mmol), **7** (0.130 g, 0.290 mmol) and tetrakistriphenylphosphine palladium(0) (0.027 g, 0.024 mmol) were placed in an oven-dried 250 mL Schlenk flask. The flask was the degassed by three vacuum/nitrogen cycles. Degassed DMF (40 mL) was then injected into the flask and the solution mixture was stirred for 12h at 100 °C under inert atmosphere. After cooling to room temperature, the reaction mixture was poured into water (300 mL) with brine (30 mL). The precipitate was filtered over Celite, washed with additional water (100 mL) and the Celite was then washed with DCM until the washings were faint blue color. Residual water was removed in a separatory funnel. DCM was removed under vacuum and the product was purified by column chromatography (30%hexane/DCM) to afford **4** as a dark blue solid (0.194 g, 81%). ^{1}H-NMR (500 MHz; $CDCl^3$): δ 9.86 (s, 1H), 8.96 (d, *J* = 4.1 Hz, 1H), 8.88 (d, *J* = 4.1 Hz, 1H), 7.67 (d, *J* = 3.8 Hz, 1H), 7.61 (d, *J* = 7.8 Hz, 2H), 7.40 (t, *J* = 7.6 Hz, 2H), 7.32-7.28 (m, 7H), 7.25 (d, *J* = 3.6 Hz, 1H), 4.04 (d, *J* = 5.9 Hz, 4H), 1.97 (m, 2H), 1.35-1.24 (m, 36H), 0.89-0.84 (m, 12H). ^{13}C-NMR (126 MHz; $CDCl_3$): δ 182.8, 161.97, 161.81, 146.5, 145.6, 143.3, 142.4, 141.4, 140.2, 139.0, 138.0, 137.7, 137.4, 136.70, 136.51, 135.6, 133.9, 129.4, 128.4, 128.2, 127.5, 126.5, 126.2, 126.0, 125.7, 124.92, 124.83, 124.5, 109.1, 108.65, 108.62, 46.6, 38.3, 32.2, 31.7, 31.4, 30.1, 28.9, 26.7, 23.5, 23.0, 14.5 HRMS calc m/z for $C_{57}H_{66}N_2O_3S_5$: 986.368, found 986.371.

A-Amide. 8 (0.100 g, 0.101 mmol) was placed in a 100 mL flask and dissolved in $CHCl_3$ (20 mL). N-benzylcyanoacetate (0.088 g, 0.505 mmol) was added, followed by piperidine (0.200 mL, 2.00 mmol). The solution was stirred at 70 °C for 4 h. After cooling to room temperature, the solution was diluted with DCM (100 mL) and washed with 1 M HCl (30 mL). The organic phase was collected and the solvent removed under vacuum. The crude was suspended in acetonitrile and filtered, to remove excess starting material. The product was purified by column chromatography (DCM, then 1%MeOH/DCM) to afford A-Amide as a dark blue solid (0. 0383 g, 33%). ^{1}H-NMR (400 MHz; $CDCl_3$): δ 8.96 (d, *J* = 4.2 Hz, 1H), 8.89 (d, *J* = 4.2 Hz, 1H), 8.37 (s, 1H), 7.62-7.61 (m, 3H), 7.42-7.27 (m, 13H), 7.24 (t, *J* = 2.9 Hz, 2H), 6.54 (t, *J* = 5.8 Hz, 1H), 4.60 (d, *J* = 5.7 Hz, 2H), 4.04 (d, *J* = 7.1 Hz, 4H), 1.97 (m, 2H), 1.35-1.24 (m, 36H), 0.85 (m, 12H). ^{13}C-NMR (126 MHz; $CDCl_3$): δ 161.90, 161.76, 160.8, 145.65, 145.55, 144.7, 143.3, 141.4, 140.1, 138.95, 138.87, 138.1, 137.51, 137.47, 136.8, 136.3, 135.6, 135.4, 133.9, 129.39, 129.24, 128.43, 128.28, 127.5, 126.44, 126.29, 126.0, 125.7, 124.92, 124.89, 124.5, 117.5, 109.1, 108.6, 99.4, 46.6, 44.9, 38.34, 38.31, 32.21, 32.19, 31.7, 31.4, 30.12, 30.09, 30.06, 28.97, 28.95, 26.7, 23.5, 23.0, 14.5 HRMS calc m/z for $C_{67}H_{74}N_4O_3S_5$: 1142.436, found 1142.435.

A-Ester. 8 (0.0940 g, 0.0952 mmol) was placed in a 100 mL flask and dissolved in $CHCl_3$ (20 mL). Benzyl-cyanoacetate (0.077mL, 0.500 mmol) was added, followed by piperidine (0.200 mL, 2.00 mmol). The solution was stirred at 70 °C for 12 h. After cooling to room temperature, the solution was diluted with DCM (100 mL) and washed with 1 M HCl (30 mL). The organic phase was collected and the solvent removed under vacuum. The crude was suspended in acetonitrile and filtered, to remove

excess starting material. The product was purified by column chromatography (5%hexane/DCM, then DCM) to afford A-Ester as a dark blue solid (0.0423g, 21%). ^{1}H-NMR (500 MHz; $CDCl_3$): δ 8.96 (d, *J* = 4.2 Hz, 1H), 8.89 (d, *J* = 4.1 Hz, 1H), 8.26 (s, 1H), 7.67 (d, *J* = 3.9 Hz, 1H), 7.62 (d, *J* = 7.2 Hz, 2H), 7.45-7.27 (m, 16H), 5.34 (s, 2H), 4.05 (d, *J* = 7.0 Hz, 4H), 1.98 (m, 2H), 1.34-1.24 (m, 36H), 0.87-0.84 (m, 12H). ^{13}C-NMR (126 MHz; $CDCl_3$): δ 162.7, 161.54, 161.40, 146.7, 146.2, 145.2, 143.0, 141.0, 139.74, 139.71, 139.4, 138.55, 138.53, 138.1, 137.2, 136.5, 135.8, 135.3, 135.1, 134.6, 133.5, 129.17, 129.08, 128.71, 128.57, 128.26, 128.11, 127.92, 127.5, 126.13, 125.99, 125.7, 125.4, 124.64, 124.56, 124.2, 115.9, 108.8, 108.3, 97.59, 97.56, 67.9, 46.3, 38.07, 38.03, 31.9, 31.4, 31.1, 29.82, 29.80, 28.67, 28.64, 26.4, 23.2, 22.7, 14.2 HRMS calc m/z for $C_{67}H_{73}N_3O_4S_5$:1143.421, found 1143.423.

Cyclic Voltammetry

S-Amide, S-Ester, A-Amide and A-Ester were drop-cast from a 10mM $CHCl_3$ solution onto the working electrode. The thin film was immersed into anhydrous acetonitrile under Argon and scanned at a rate of 100 mV/s using 100 mM tetrabutylammonium hexafluorophosphate (NBu4PF6) in acetonitrile as the supporting electrolyte. The ferrocene/ferrocenium (Fc/Fc+) redox couple was used as an external standard and was assigned an absolute energy level of -4.8 eV vs. vacuum.[4] Potential is reported vs. $Ag/AgNO_3$ (non-aqueous reference electrode). The HOMO levels were determined by the equation HOMO = -4.8 + ($E_{oxFc/Fc+}$ - E_{oxM}) where $E_{oxFc/Fc+}$ and E_{oxM} are the onset oxidation potentials of ferrocene and M, where M = S-Amide,S-Ester, A-Amide and A-Ester. The LUMO levels were obtained by the equation LUMO = -4.8 + ($E_{oxFc/Fc+}$ - E_{redM}), where E_{redM} are the onset reduction potentials of M. The CV traces for all four molecules show quasireversible oxidation waves in the region of 0.5-1 V. The reduction potentials occur in the -1 V region and present reversible behavior for all four molecules, but S-Amide presented a pre-reduction wave that made assigning a reduction potential difficult; for this reason, the difference in Eg reported in the manuscript for S-Amide and S-Ester is approximately 0.4 eV, even though their onset absorption would seem to indicate they should have nearly identical values for Eg.

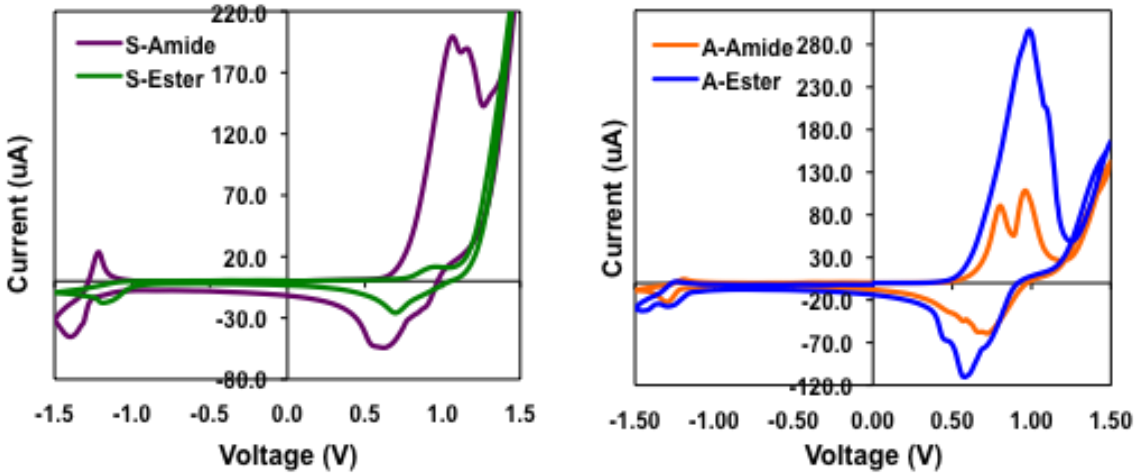

Figure S1. Cyclic voltammograms of S-Amide, S-Ester, A-Amide and A-Ester.

Infrared Spectroscopy

Films of S-Amide, S-Ester, A-Amide, A-Ester, precursor **4** and N-benzyl-2-cyanoacetamide were cast from a 10 mM $CHCl_3$ solution on a Ge crystal. Films of blends were prepared by drop-casting 10mg/mL chlorobenzene solutions of S-Amide, S-Ester, A-Amide and A-Ester with PCBM in a 1:1 weight ratio onto a Ge crystal. Although drop-casting blends does not reproduce device conditions exactly, we feel the results shown can be extrapolated to spin-coated conditions with sufficient accuracy. Attenuated total reflectance (ATR) spectra were offset for clarity. Figure S2 shows the comparison between S-Amide and S-Ester and A-Amide and A-Ester. Hydrogen bonding can be

detected by FTIR when the C=O and N-H stretching vibrations shift to lower wavenumbers when hydrogen bonding is present. The C=O stretch could not be unambiguously assigned, as three peaks of similar intensity appear in the region of 1650 cm^{-1}. The N-H stretching peak is the weak peak at 3440 cm^{-1} for S-Amide and 3360 cm^{-1} for A-Amide. The relatively low signal is mainly due to N-H being a single bond, among the much more abundant C=C and C-H stretching signals (from thiophene and alkyl tails, respectively). Close up views of the amide region are shown in Figure S2, where it can be seen that the ester versions show no signal in that region. S-Ester was a special case in the sense that it presented a broad shoulder in the amide region, which we attribute to abnormal background subtraction caused by the poor film quality when drop-cast from $CHCl_3$; in the later films from chlorobenzene (with PCBM), where the quality of the film was slightly better, the shoulder disappears. As mentioned in the text, to investigate the effect of conjugation on the strength of hydrogen bonding, S-Amide and A-Amide were compared with the precursors **4** and *N*-benzyl-2-cyanoactetamide, respectively. Precursor **4** shows the N-H stretching as a broad peak at 3300 cm^{-1} and *N*-benzyl-2-cyanoacetamide at 3310 cm^{-1}. The close up views show the precursors 4 and N-benzyl-2-cyanoacetate having the N-H stretch at lower wavenumbers than S-Amide and A-Amide, respectively, which is a sign that upon conjugation to a chromophore, the strength of the hydrogen bonding ability decreases. Lastly, the blends with PCBM in Figure S6, more clearly shown in Figure S7, show the N-H signal unchanged upon mixing donor and acceptor, which is a good indication of hydrogen bonding for A-Amide, and as mentioned in the manuscript, no significant hydrogen bonding for S-Amide. Since the blends were drop-cast from chlorobenzene, they had to be air dried, which increased the CO_2 signal, as can be seen in the region of 2360 cm^{-1} in the PCBM blends. Although we expected all amides to be able to hydrogen bond, we believe S-Amide was not able to do so because the π-π stacking dominated the assembly; also, the termini alkyl tails were branched, and being flexible, could have interfered with the otherwise favorable hydrogen bonding.

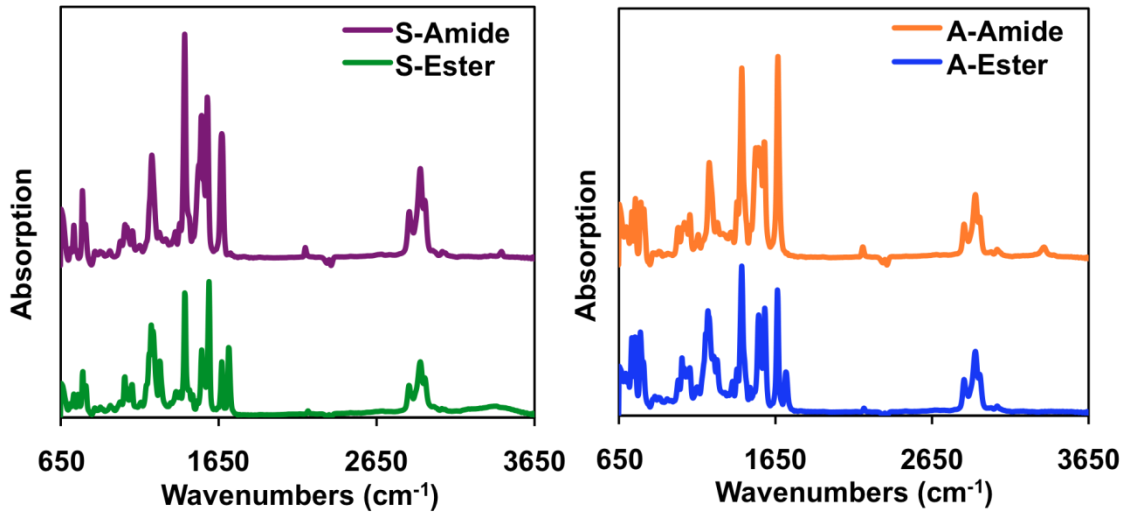

Figure S2. Infrared spectra of S-Amide and S-Ester (left) and A-Amide and A-Ester (right).

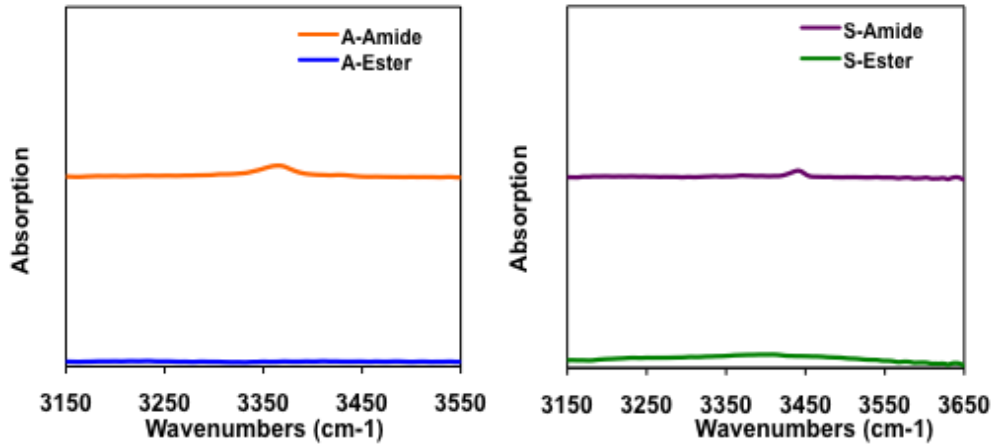

Figure S3. Close-up view of amide region of Figure S2.

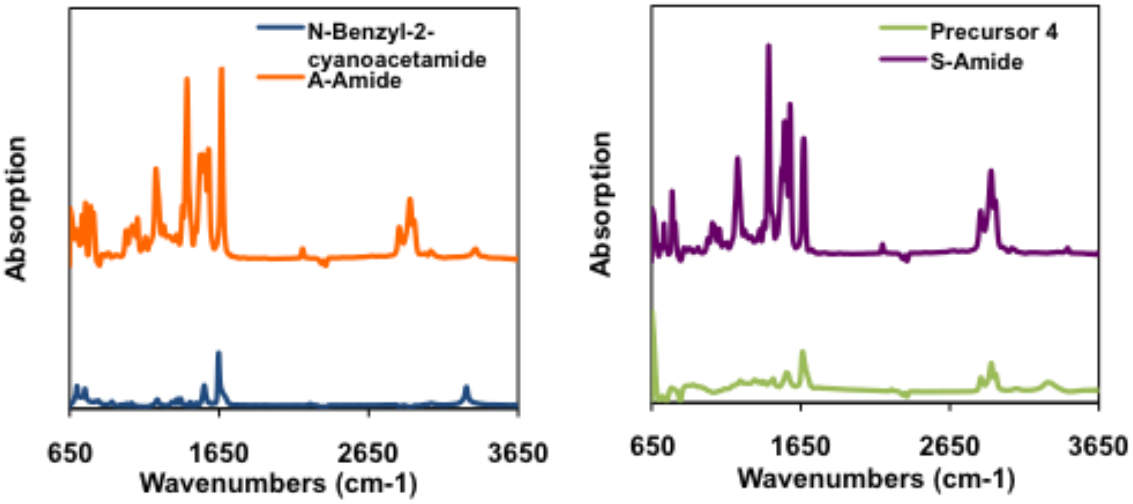

Figure S4. Infrared spectra of A-Amide with N-benzyl-2-cyanoacetate (left) and S-Amide with precursor **4** (right).

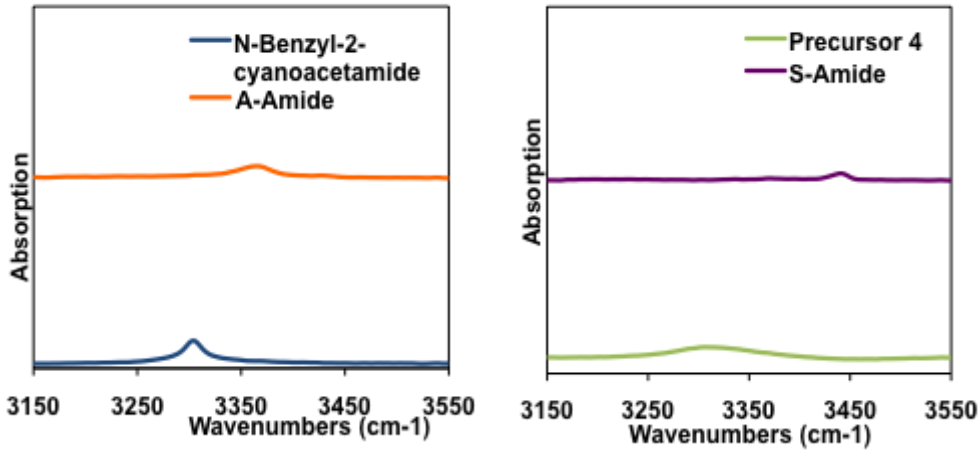

Figure S5. Close-up view of amide region of Figure S4.

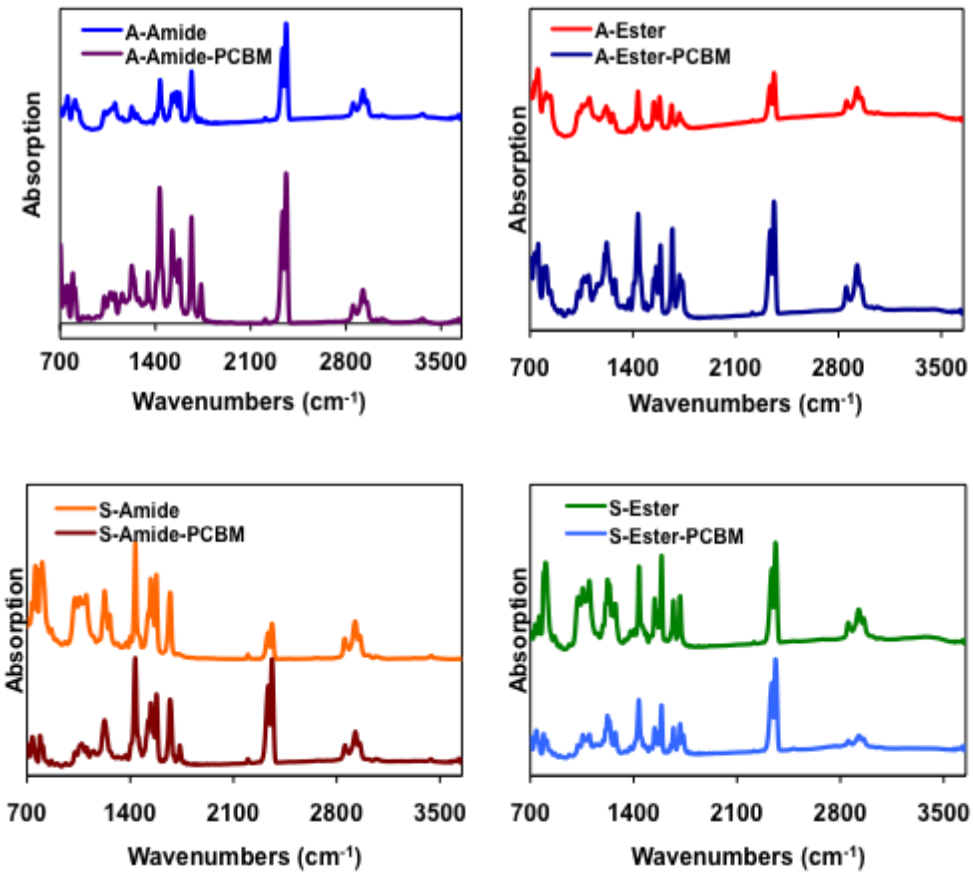

Figure S6. FITR spectra of A-Amide (top left), A-Ester (top right), S-Amide (lower left) and S-Ester (lower right). The peaks in the region of 2360 are due to high amounts of CO_2, as these measurements are done in air.

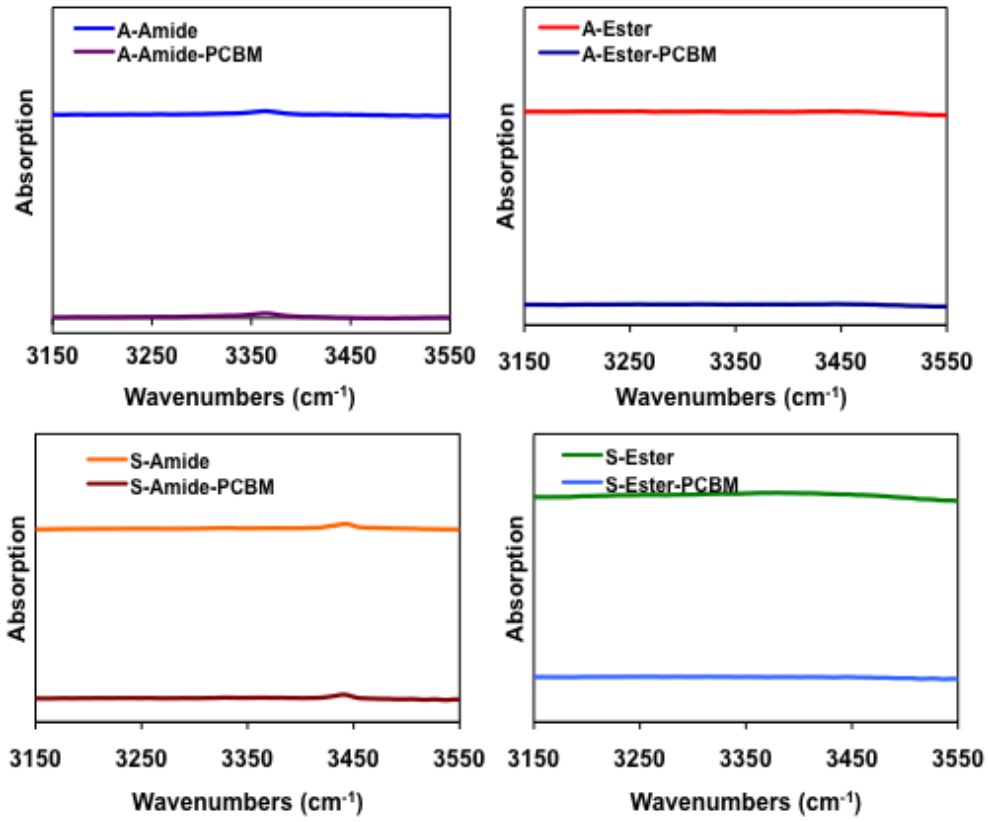

Figure S7. Close up view of amide region of all four molecules in Figure S6.

UV-Vis Spectroscopy

Extinction coefficient was determined by UV-Vis in standard solutions of the four molecules at 0.1, 0.05,0.025 and 0.0125 mM in $CHCl_3$, and the average of the four spectra was plotted on the left of Figure S8; film studies were done using two conditions, drop-casting from 10mM $CHCl_3$ solutions, to test the maximum degree of aggregation (shown in Figure 1 in the manuscript), and spin-coating with PCBM under device conditions with the maximum PCE, shown in Figure S8 in the right.

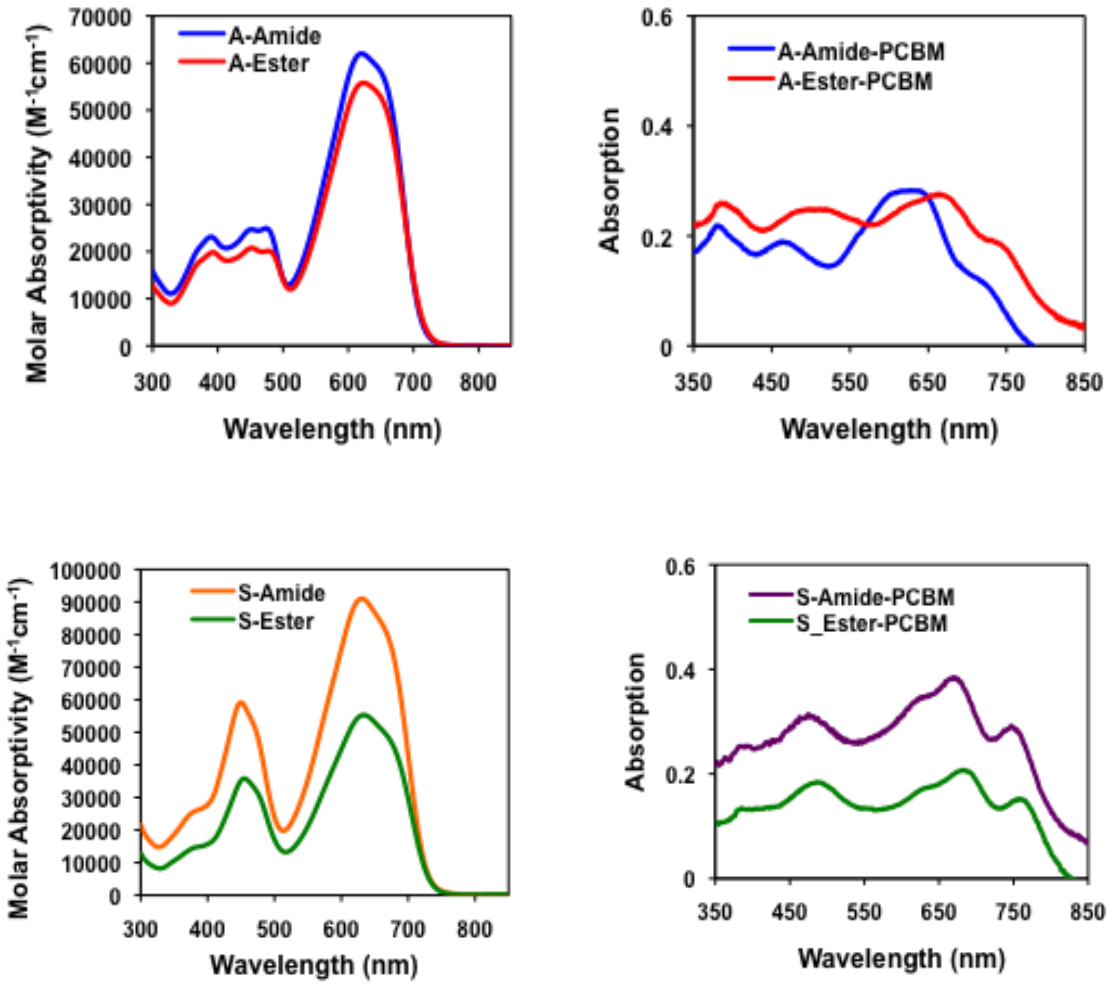

Figure S8. Absolute absorption of the four molecules in $CHCl_3$ (left) and unnormalized film absorption with PCBM under maximum PCE conditions (right).

Devices

Experimental conditions for active later deposition such as solvent, concentration and solvent composition were optimized. Pre-patterned indium-doped tin oxide (ITO) on glass was used as the transparent bottom electrode. The ITO was scrubbed with soapy water and cleaned by ultrasonicating sequentially in hexanes, soapy water, water, and a 1:1:1 solution of acetone/methanol/2-propanol. The electrode was then blown dry in a N_2 stream and transferred into a N_2 glovebox (O_2 and H_2O < 0.1 ppm). Before active layer coating, MoOx (10 nm) was thermally evaporated on ITO surface as the interfacial layer. Bulk heterojunction photovoltaic devices were fabricated from blends of donor small molecule and acceptor phenyl-C71-butyric acid methyl ester ($PC_{71}BM$). In the optimized conditions, donor/acceptor ratio is fixed to 1:1, with a total solution concentration of 22 mg/ml in chlorobenzene. Films were cast by spin-coating at 2000 rpm in the glovebox for 60 s and annealed on a hot plate at 100°C for 5 minutes. Total organic layer thickness ranged from 60-70 nm as determined by AFM. Devices were completed by thermally evaporating 1 nm of LiF then 100 nm of Al through a shadow mask at 1 x 10^{-6} mbar to yield devices of 4 mm^2 in area and sealed with a UV-curable epoxy if needed. The devices for space-charge-limited-current (SCLC) measurements were fabricated with a similar procedure. Hole transport layer were replaced with PEDOT:PSS (Clevios P VP Al 4083) and the top electrode is replaced with Au (50 nm) rather than LiF/Al in order to suppress electron injection.

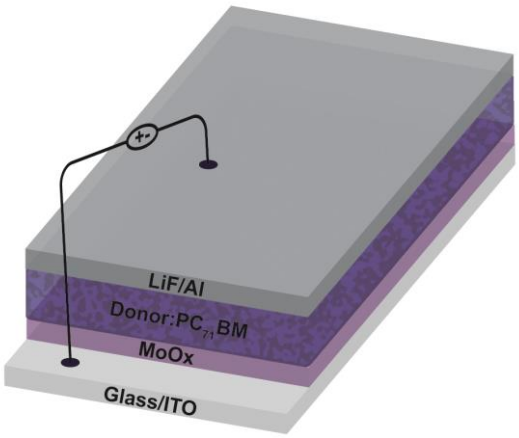

Figure S9. Schematic illustration of solar cell architecture used in this study

J-V curves of symmetric devices are given in Figure S6. Nitrobenzene (NB) and 1,8-diiodooctane (DIO) were used as a solvent additive for symmetric devices and solar cell parameters are presented in Table S2. Even though there is some improvement in device performance (especially for S-Amide) with the addition of solvent additives, PCE of the solar cells still remained under 1%.

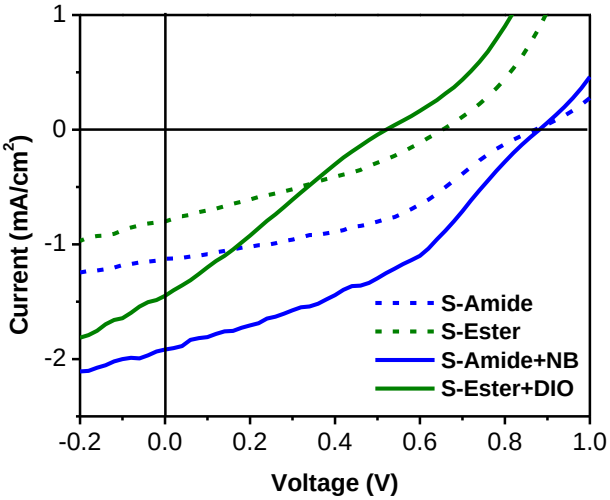

Figure S10. J-V characteristic of optimized solar cells of symmetric molecules with $PC_{71}BM$ under illumination

Table S2. Optimized solar cell results of symmetric molecules with solvent additives. [a]

Device	V_{OC}(V)	J_{SC}(mA/cm^2)	FF (%)	PCE (%)
S-Amide+NB	0.87 ± 0.03	1.9 ± 0.1	38 ± 1	0.61 ± 0.05
S-Ester+DIO	0.50 ± 0.03	0.9 ± 0.4	18 ± 5	0.09 ± 0.06

[a]Average performance of four devices.

J-V curves of additional asymmetric devices are given in Figure S7. When DIO is used with A-Amide and NB is used for A-Ester, resulting solar cell efficiency becomes even less than that the devices that don't have any solvent additive (Table S3).

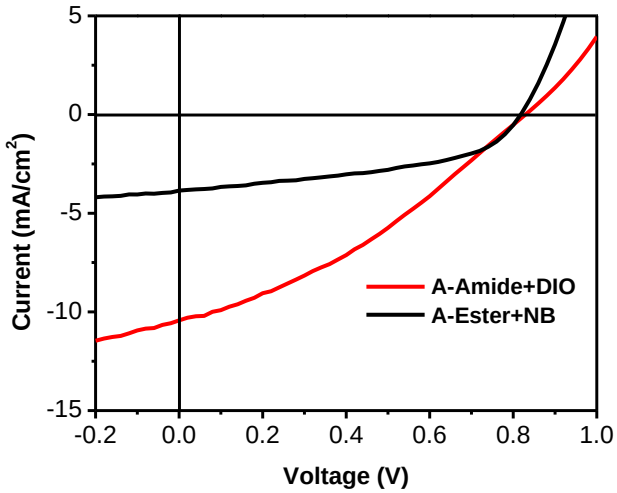

Figure S11. J-V characteristic of optimized solar cells of asymmetric molecules with different solvent additives under illumination.

Table S3. Solar cell results of asymmetric molecules with different solvent additives.[a]

Device	V_{OC}(V)	J_{SC}(mA/cm^2)	FF (%)	PCE (%)
A-Amide+DIO	0.83 ± 0.01	9.7 ± 0.1	37 ± 2	2.95 ± 0.14
A-Ester+NB	0.81 ± 0	3.6 ± 0.2	47 ± 1	1.37 ± 0.08

[a]Average performance of four devices.

Hole mobility were estimated using the data showed in Figure S6 with the following equation:

$$J = \frac{9}{8}\frac{\varepsilon\mu_0}{L^3}V^2 \quad (1)$$

where J is current, ε is relative permittivity of the material (assumed as 3 for most organic materials), L is the thickness of the film, V is the applied voltage and μ is the mobility. For the absolute voltage, the voltage drop across the ITO due to series resistance (V_{RS}) and built in voltage (V_{BI}) was subtracted from the applied voltage.[5] The only remaining unknown L, the thickness of active layer, was measured with AFM (Table S4). These results were used to determine the hole mobility of each active layer.

Table S4. Thicknesses of active layer blends measured with AFM

Sample	Thickness (nm)
A-Amide	70
A-Amide + NitroBenzene	100
A-Ester	75
A-Ester +DIO	90

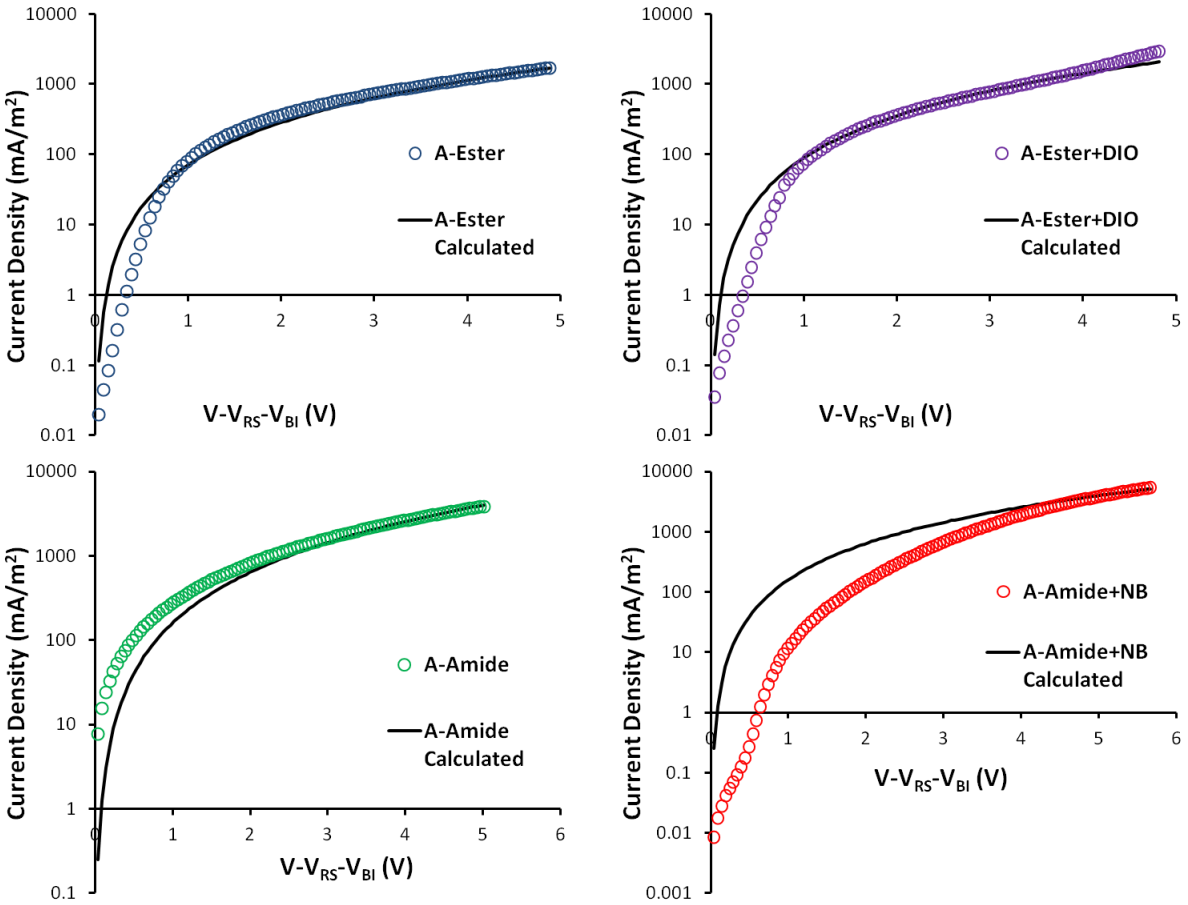

Figure S12. Experimental dark-current densities of A-Ester and A-Amide blends measured at room temperature in a hole only device configuration (empty marker). Experimental dark-current densities superimposed with curves calculated with SCLC theory (solid line)

Microscopy

AFM measurements were either performed on the fabricated solar cell device or on a separate sample prepared with the same spin coating parameters used for device on a freshly cleaved mica substrate. AFM images are processed with WSxM software.[6] Samples for conventional transmission electron microscopy (TEM) were prepared by fishing the active layer that floats on water onto a cupper TEM grid. To float the active layer in water a sacrificial PEDOT:PSS layer is coated on a glass and active layer is spin coated on PEDOT:PSS layer.

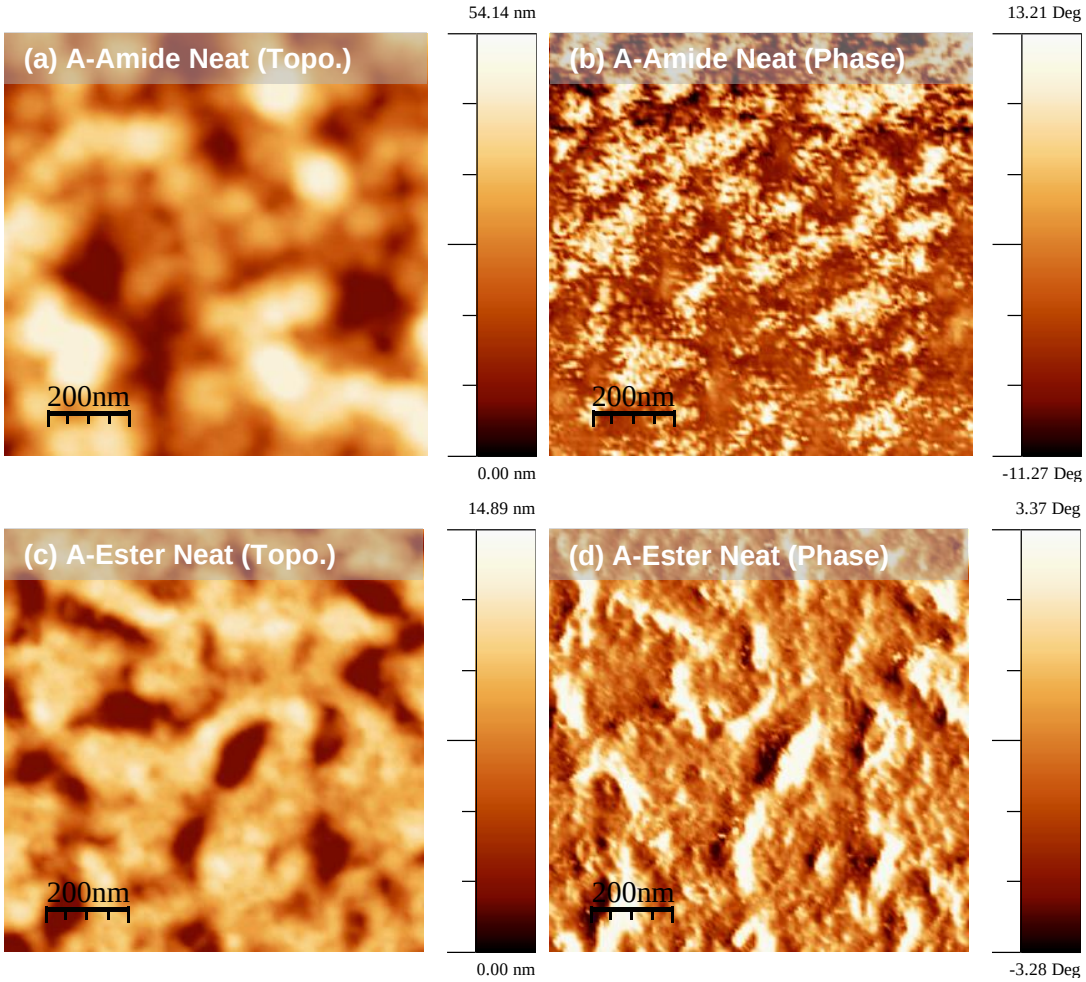

Figure S13. AFM topography (a,c) and phase (b,d) images of A-Amide and A-Ester neat films respectively, casted on mica from chlorobenzene and annealed at 100°C for 5 minutes.

GIXD

GIXD samples were prepared on silicon chips by spin coating donor/acceptor solutions with the same conditions used for devices. All samples were illuminated with X-ray for a short period of time (1-2 s) with an incident angle of 0.2°.

GIXD of films from symmetric molecules are given in Figure S14. For both S-Amide and S-Ester, (100) rings with higher order reflections can be seen. This ring is characterized for alkyl-alkyl stacking distance. In addition, (010) ring with a characterized π-π stacking distance (0.37 nm) can be observed for both symmetric molecules. Same peaks can also be observed after blending the molecules with $PC_{71}BM$. GIXD of neat films of asymmetric molecules are given in Figure S15. Here for A-Amide, only one order of (100) ring is seen indicating weak alkyl-alkyl stacking and there is not a (010) ring that is associated to π-π stacking. On the other hand, for A-Ester film (100) ring appears with higher order reflections and (010) ring can also be observed clearly. Overall, A-Ester film displays a better crystallinity than A-Amide film.

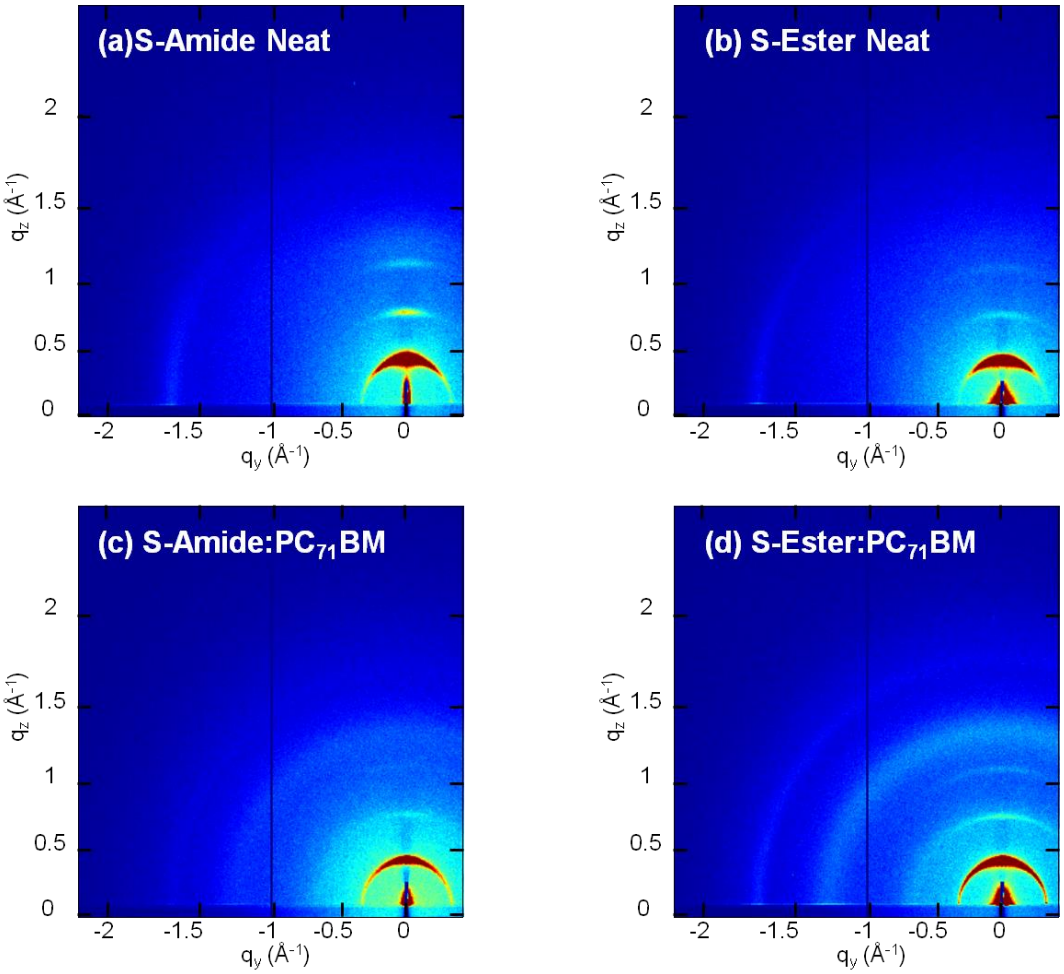

Figure S14. GIXD of symmetric molecules for neat films (a, b) and donor:$PC_{71}BM$ blends (c, d).

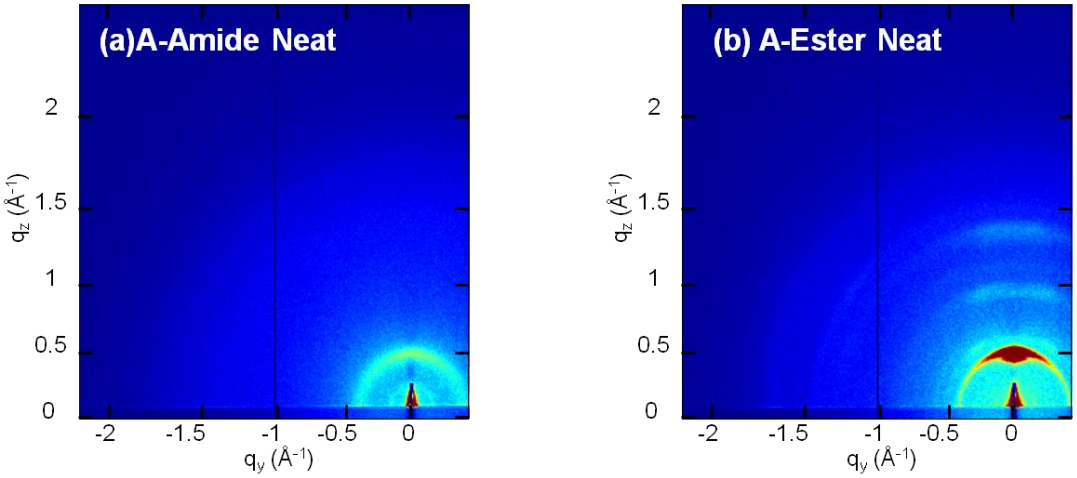

Figure S15. GIXD of asymmetric molecules for neat films (a, b)

Orientational distribution of the crystallographic features can be quantitatively described in terms of an orientational order parameter ***S*** (Herman's orientation parameter). Where separate orientational parameters $f_{\perp}$ and $f_{//}$ used to represent the orientation of polymeric crystallites, respectively, along the plane of the film surface and along the axis normal to the surface are determined from the geometrically corrected scattered intensity.[7] ***S*** can be calculated by knowing $f_{\perp}$ (eq.1) which is calculated with the cosine function (eq. 2) as given below.

$$S = \frac{1}{2}\left(3f_{\perp} - 1\right) \tag{2}$$

$$f_{\perp} = \left\langle \cos^2\chi \right\rangle = \frac{\int_0^{\pi/2} I(\chi)\left(\cos^2\chi\right)\left(\sin\chi\right)d\chi}{\int_0^{\pi/2} I(\chi)\left(\sin\chi\right)d\chi} \tag{3}$$

From a practical perspective, ***S*** is a quantity that varies between -0.5 and 1, where value of 1 (-0.5) indicates parallel (orthogonal) orientation of the normal of a crystallographic plane relative to substrate normal. Conversely, a completely isotropic distribution of the crystallographic planes leads to an ***S*** value of 0.

References

1. Jiang, Z.; Li, X.; Strzalka, J.; Sprung, M.; Sun, T.; Sandy, A. R.; Narayanan, S.; Lee, D. R.; Wang, J. *Journal of Synchrotron Radiation* **2012,** *19* (4), 627-636.

2. Lee, O. P.; Yiu, A. T.; Beaujuge, P. M.; Woo, C. H.; Holcombe, T. W.; Millstone, J. E.; Douglas, J. D.; Chen, M. S.; Fréchet, J. M. J. *Adv. Mater.* **2011,** *23* (45), 5359-5363.

3. Denat, F.; Gaspard-Iloughmane, H.; Dubac, J. *ChemInform* **1993,** *24* (7), 954-956.

4. Pommerehne, J.; Vestweber, H.; Guss, W.; Mahrt, R. F.; Bassler, H.; Porsch, M.; Daub, J. *Adv. Mater.* **1995,** *7* (6), 551-554.

5. Mihailetchi, V. D.; Xie, H. X.; de Boer, B.; Koster, L. J. A.; Blom, P. W. M. *Adv. Funct. Mater.* **2006,** *16* (5), 699-708.

6. Horcas, I.; Fernandez, R.; Gomez-Rodriguez, J. M.; Colchero, J.; Gomez-Herrero, J.; Bario, A. M. *Review of Scientific Instruments* **2007,** *78* (8), 013705-1--013705-8.

7. Chen, W.; Nikiforov, M. P.; Darling, S. B. *Energy Environ. Sci.* **2012,** *5* (8), 8045-8074.